Long waves in the equatorial Pacific Ocean. *EOS*, 66, 154-155.

Wallcraft, A., 1991: *The Navy Layered Ocean Model Users Guide*. NOARL Report No. 35, Stennis Space Center, MS.

Wimbush, M., S.M. Chiswell, R. Lukas, and K.A. Donohue, 1990: Inverted echo sounder measurement of dynamic height through an ENSO cycle in the central equatorial Pacific. *IEEE J. Oceanic Eng.*, 15, 380-383.

Wyrtki, K., 1974: Sea level and seasonal fluctuations of the equatorial currents in the western Pacific Ocean. *J. Phys. Oceanogr.*, 4, 91-103.

Xiaoli Zhu, Mark Wimbush, and Kathleen A. Donohue
Graduate School of Oceanography
University of Rhode Island
Narragansett, RI 02882, U.S.A.

Stephen M. Chiswell and Roger Lukas*
JIMAR, University of Hawaii
1000 Pope Road
Honolulu, HI 96822, U.S.A.

Laury Miller
NOAA/NOS Geosciences Lab, NOES11
6001 Executive Boulevard
Rockville, MD 20852, U.S.A.

Harley E. Hurlburt
Naval Research Laboratory, Code 7323
Stennis Space Center, MS 39529, U.S.A.

**Present address:*
New Zealand Oceanographic Institute NIWAR
P.O. Box 14-901, Kilbirnie
Wellington, New Zealand

Dissipation in a Pacific Equatorial Long Wave Model

Joël Picaut
Christophe Menkes
Jean-Philippe Boulanger --

Introduction

The importance of long equatorial waves in the development of El Niño has been widely recognized since the seminal works of Wyrtki (1975) and McCreary (1976). Equatorial-ocean linear models, forced by observed winds, have been quite successful in reproducing the major sea-level signature of El Niño (see, e.g., Busalacchi *et al.*, 1983). This event is the result of an intrinsic coupling between tropical ocean and atmosphere (El Niño-Southern Oscillation, or ENSO), and both simple and complex coupled ocean-atmosphere models have been developed to understand the phenomenon (McCreary and Anderson, 1991; Neelin *et al.*, 1992). Analyses of model solutions have led to several interesting ENSO theories, such as the delayed-action oscillator (Suarez and Schopf, 1988; Battisti and Hirst, 1989), in which equatorial Rossby and reflected Kelvin waves are important. Unstable coupled ocean-atmosphere modes therefore may be at the origin of ENSO. According to Wakata and Sarachik (1991), these modes are sensitive to the choice of Rayleigh friction.

Dissipation in the form of Rayleigh friction was introduced by Gill (1980) in an equatorial long-wave model. For a multiple-mode linear model, friction is usually taken as a vertical-mode dependent parameter (if possible based on physical assumptions) to allow separation into vertical modes (McCreary, 1981). Gent *et al.* (1983) discuss the equivalence of horizontal and vertical damping with Rayleigh friction and its vertical-mode dependence. Through a model best fit of the observed semiannual zonal current oscillation in the equatorial Indian Ocean, the same authors found a first-vertical-mode decay time of two years. Without a better estimate of damping, many modelers have used a similar value for the Rayleigh-friction coefficient.

The purpose of our study is to estimate the Rayleigh-friction coefficient in an equatorial long-wave model, constraining sea-level results to best fit three independent observed sea-level data sets (tide gauges, moorings and GEOSAT). Following the results of Busalacchi and Cane (1985), where the addition of the third and fourth vertical modes does not add any constructive information to their model/data intercomparison, our study is done using two vertical modes, and without any *a priori* hypothesis on the dependence of the friction coefficient on mode number.

Data

The longest sea-level data set (1975-89) used in this study is deduced from daily means of tide-gauge measurements at 14 islands, situated mostly in the western Pacific (Figure 1). Between instrumental uncertainties, island and barometric effects, the error in sea-level estimates is of the order of a few centimeters.

Daily mean, surface dynamic-height fields, relative to 500 db, are derived from the temperature sensors of nine TOGA-TAO moorings and three current meter moorings (McPhaden and Hayes, 1990), using Levitus (1982) mean TS relations. Most of the dynamic-height time series cover the 1986-91 period, except at 0°-140°W and 0°-110°W, where they start in November 1983. The significance of these open-ocean time series is altered by several gaps and technical constraints (such as the use of a reference level, mean TS relations, and inadequate vertical temperature sampling), which probably result in error ranges at least equal to those of the tide-gauge measurements.

The GEOSAT altimetric sea-level data, resulting from the geodetic and exact-repeat missions, cover the April 1985 - October 1989 period over most of the tropical Pacific (Figure 1). There is a gap in the data from 30 September 1986 to 8 November 1986 between the two different missions, and there is serious data degradation after May 1989. This data set was built on a 8° longitude x 1° latitude grid and interpolated to daily values. Detailed information about data combination within the two missions, their corrections, and their processing can be found in Miller and Cheney (1990) and Cheney *et al.* (1991a). The improved water-vapor and orbit corrections result in an rms difference between monthly GEOSAT and island sea level of 3 to 4 cm (Cheney *et al.*, 1991b).

Model

The model is linear and forced by the observed wind-stress fields over the period 1961-91, and is described in detail in Cane and Patton (1984). Briefly, the linear shallow-water equations are solved on an equatorial β-plane, subject to the low-frequency long-wave approximation. Variables are calculated every 5 days and are located on a staggered grid of 2° longitude by 0.5° latitude within the model boundaries (Figure 1). The forcing is derived from the 2° x 2° monthly pseudo-stress FSU (Florida State University) wind product (Goldenberg and O'Brien, 1981) through a drag coefficient C_D, and is then linearly interpolated to the model time and space grid. Changing the drag coefficient results in a proportional change in the amplitude of model solutions. These solutions are generated for the first and second vertical modes calculated from a specific vertical density profile. The total sea-level height field is found by summing the individual contribution of these two modes. Model wind-stress projections and internal-wave speeds are calculated from several types of vertical density profiles. Levitus (1982) profiles, representative of the mean condition along the Pacific equator, and instantaneous profiles taken during the ALIZE2 cruise (Eldin *et al.*, 1992) are used.

Model-data Adjustment

The linear model forced by FSU monthly wind stress cannot reproduce oceanic phenomena with periods lower than two months. Therefore a 95-day Hanning filter is used in order to remove the observed 40-60 day and 20-30 day waves from the sea-level data. A Levitus density profile of the central Pacific is selected first. The corresponding phase speeds are $c_1 = 2.45$ m s^{-1} for mode 1, and $c_2 = 1.51$ m s^{-1} for mode 2. Our approach is to find the optimal fit between model and observed series by tuning the drag coefficient (C_D) and the decay times for the first (T_1) and second (T_2) vertical modes.

For the purpose of our study, we define *cor* as the global correlation coefficient (sums are made on space and time) and *rms* as the global rms difference between model and observations, both scaled to the global standard deviation of the observed series. We also define the global scaled standard deviation (σ_{sc}) as the ratio of the global standard deviations of the modeled and observed series (i.e., the ratio of their amplitudes). Since C_D directly acts on the amplitude of the model, we can write

$$\sigma_{sc} = \alpha C_D, \qquad (1)$$

where α is a function only of T_1 and T_2. Basic algebra shows that the quantities *cor*, Δrms, and σ_{sc} are dependent through the relation

$$(\Delta rms)^2 = \sigma_{SC}^2 - 2\sigma_{sc} cor + 1. \qquad (2)$$

Since *cor* is only a function of T_1 and T_2, Δrms is a function of T_1, T_2, and C_D.

The best fit between the modeled and observed series is achieved for maximum of *cor* and minimum of Δrms. For fixed values of T_1 and T_2 (i.e., for a given *cor*), the minimum of Δrms in (2) is equal to $\sqrt{1-cor^2}$ when $\sigma_{sc} = cor$. According to (1), the only way to get $\sigma_{sc} = cor$ is to tune C_D so that $C_D = cor/\alpha$, which is now a function of (T_1,T_2). In order to find the maximum of *cor*, the calculation is then reiterated for T_1 and T_2, varying from very viscous (11 days) to inviscid (32 years) cases. At the maximum of *cor*, Δrms, which is equal to $\sqrt{1-cor^2}$, reaches its absolute minimum.

Figure 2 presents, for fixed values of T_1, T_2, and C_D, the spatial distribution of the correlation coefficients in time between model and GEOSAT sea level. It shows that the lowest correlations are mostly located around the ITCZ (Inter-Tropical Convergence Zone) and SPCZ (South Pacific Convergence Zone). In order for the global correlation coefficient to be significant, the following method is used. At each data point, the maximum of correlation in time is estimated among all the values of correlation in time calculated for various couples (T_1, T_2). If this maximum of correlation is not significant at 90% (following the significance method of Sciremammano, 1979), the corresponding data point is not taken into account in further calculations. With this criterion at hand, all tide gauges and moorings and 80% of GEOSAT grid points are retained.

The global correlation coefficient and drag coefficient are shown in Figure 3 as functions of T_1 and T_2 for each data set. The maximum of correlation coefficient gives close (T_1,T_2) for tide gauges and GEOSAT. For tide gauges, T_1 is around 7 months and T_2 is lower than 4 months; for GEOSAT, T_1 is around 5 months and T_2 is lower than 2 months. Results for the moorings are somewhat different, with a maximum of correlation coefficient for T_1 around 2 months and for T_2 around 4 months.

If one assumes that higher vertical modes will experience more frictional damping, T_2 should be lower than T_1, which is not the case for the mooring data. One reason for this discrepancy might be that surface dynamic height relative to 500 db does not take into account all the vertical information of the first baroclinic mode and probably gives too much weight to the second mode. Another reason is that the mooring data are restricted to specific locations. To test the latter hypothesis, a correlation analysis was performed with GEOSAT data series interpolated to the mooring positions. The results for the maximum of correlation are the *same* as the global GEOSAT results. Thus, we conclude that the discrepancy is due to the mooring locations, and therefore give more credit to the tide gauge and GEOSAT results. In the following, then, we use decay times of 5 months for the first mode and 3 months for the second mode. From this estimation of (T_1,T_2), the right panel of Figure 3 gives a drag coefficient of 1.8, 1.5, and 1.4 x 10^{-3}, respectively, for tide gauges, moorings, and GEOSAT. Finally, this method allows an estimate of a mean C_D of 1.6 x 10^{-3}.

All of the previous analyses were performed with a specific Levitus vertical density profile from the central Pacific. It is important to test the sensitivity of the results to the choice of profile. Five other mean Levitus profiles and five instantaneous profiles, taken during the ALIZE2 cruise, were selected all along the equator. Correlation analyses with these various profiles show no significant difference in the decay-time results. The extreme values of the first vertical mode phase speed among these profiles are 2.1 m s^{-1} and 2.8 m s^{-1}. Given our estimation of decay times, the phase differences induced in the model solutions by these extreme phase speeds cannot be significantly resolved by the use of monthly FSU wind stress, which results in an uncertainty of at least 15 days.

Discussion and Conclusions

Sea level determined from a linear, equatorial long-wave model are correlated

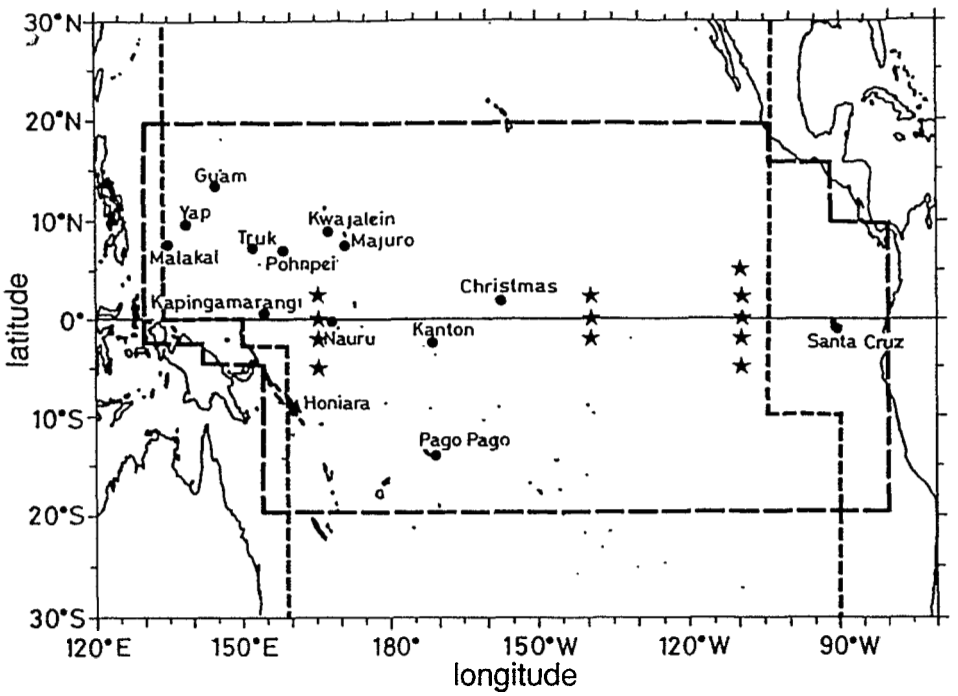

Figure 1. Location of moorings (stars) and island tide gauges (black dots). Broken lines represent the limits of available GEOSAT data, and long broken lines denote the model boundaries.

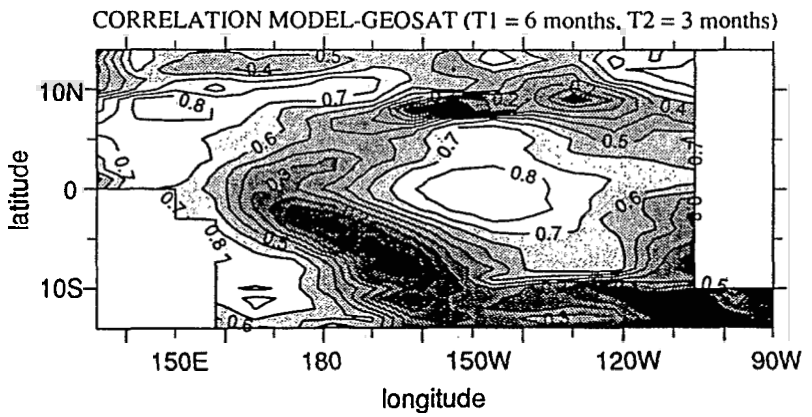

Figure 2. Correlation coefficients in time between modeled and GEOSAT sea-level time series for fixed values of T_1, T_2, and C_D.

with three independent *in situ* measurements (tide gauges, moorings, and GEOSAT) in order to estimate Rayleigh-friction coefficients (i.e., decay times) of the first and second vertical modes. The method of comparison is based on the determination of the maximum of correlation coefficients and simultaneous minimum of rms difference between modeled and observed time series, which in addition results in the estimation of a drag coefficient. Our results lead us to conclude that the best-fit parameters are $T_1 = 5$ months, $T_2 = 3$ months, and $C_D = 1.6 \times 10^{-3}$.

All of our previous correlations were done with modeled and observed series filtered with a 95-day Hanning filter. A test with several low-pass filters (up to 1 year) reveals a small shift in the first-mode decay time result (up to 7 months for a 1-year filter). This small tendency may reflect that low-frequency phenomena are less damped than high-frequency ones. Therefore, we suggest that $T_1 = 6$ months and $T_2 = 3$ months may be more accurate estimates for the decay time scales.

For these values of T_1 and T_2, *cor* and Δrms are respectively 0.63 and 0.78 for tide gauges, 0.64 and 0.77 for moorings, and 0.62 and 0.78 for GEOSAT. The mean correlation could indicate that only 40% of the observed variance is explained by the model. It must be pointed out, however, that the sea-level data used in this study are noisy (cf. data section): correlation between GEOSAT and tide gauges and between GEOSAT and moorings indicates that only 68% of the variance is common to all three data sets.

We find that the decay time of mode 2 is lower than that of mode 1 for the tide gauges and GEOSAT data. The test with various density profiles shows that, except for the sharp profile taken during the ALIZE2 cruise in the far-eastern equatorial Pacific, the first mode is the dominant signal in the modeled sea-level amplitude (two-thirds). The broad range of second-mode decay time, suggested by the shape of Figure 3 around the maximum of correlation coefficient, does not allow us to extract a well-defined dependence between decay time and mode number, and shows that the second mode has little influence on the phase of the total (mode 1 + 2) sea-level signal.

Because of the Rayleigh friction, free waves in the linear solutions decay exponentially in time, the corresponding decay times representing the lifetime of free equatorial waves. Our dissipation results, estimated from the best fit between simulated and *in situ* sea-level series, probably include some of the ocean physics missing in the linear model (e.g., damping of equatorial waves by mean currents). Thus, processes affecting dissipation in more complex models and the real ocean may be represented in our study by smaller decay times.

Since the Rayleigh friction coefficient commonly used in linear models is (2.5 years)$^{-1}$, our results suggest that dissipation in the equatorial ocean may be stronger than expected. Consequently, multi-reflections of equatorial waves on meridional boundaries may be impossible. Moreover, none of the amplitude of an extra-equatorial Rossby wave generated in the central Pacific may

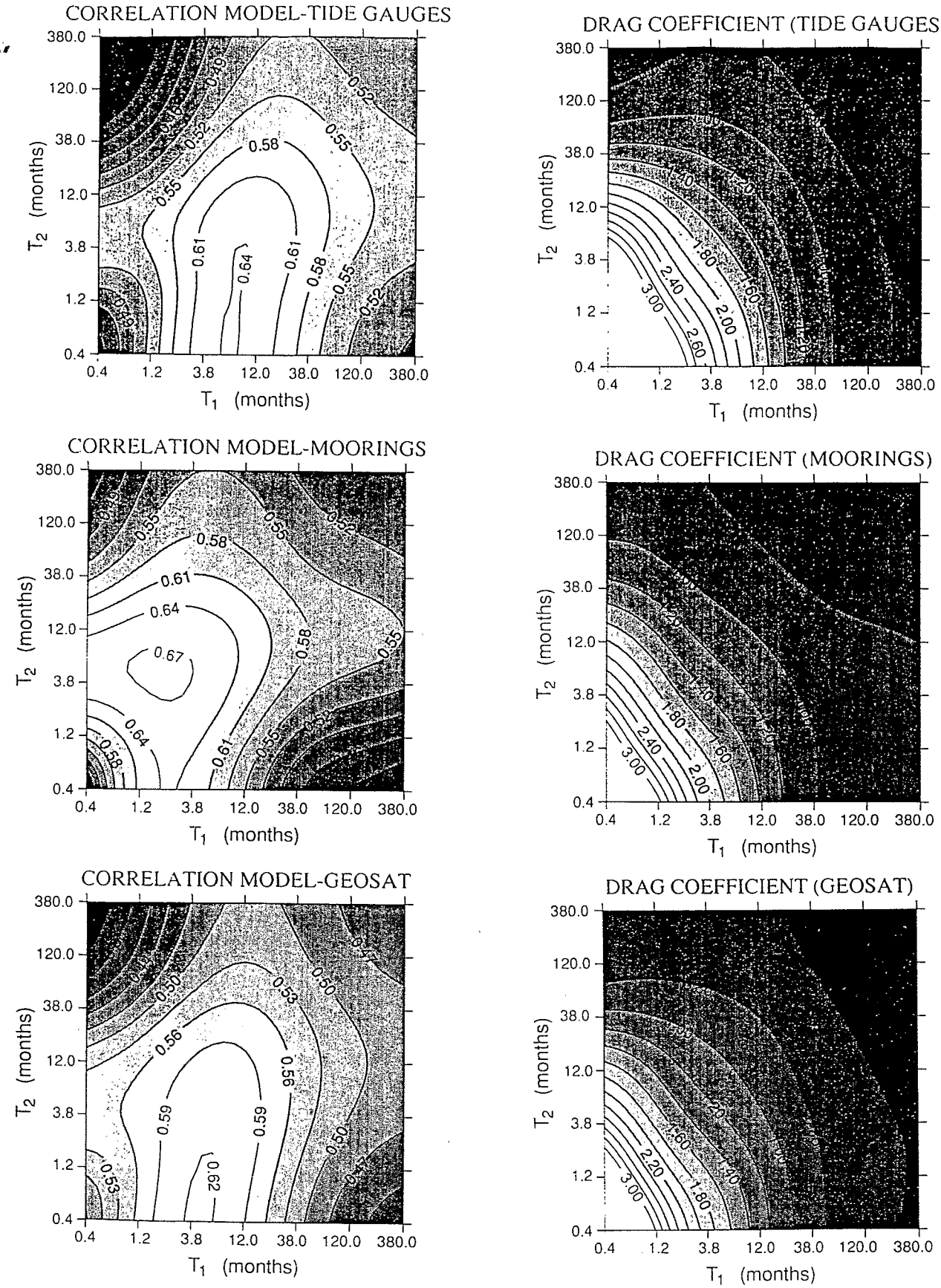

Figure 3. Global correlation coefficients (left panel) and drag coefficients (right panel) calculated from comparison between modeled and (top to bottom) island tide gauge, mooring, and GEOSAT sea-level series. The contour interval is every 0.03 for the correlation coefficients. Logarithmic scales on x-y axes are used for clarity.

reach the western boundary to be reflected as an equatorial Kelvin wave. In examining the parameter dependence of their coupled atmosphere-ocean basin mode, Wakata and Sarachik (1991) found that the limit of the oceanic Rayleigh friction, between oscillatory and non-oscillatory model solutions, is about (4 months)$^{-1}$. Our Rayleigh friction estimate of (6 months)$^{-1}$ for the first vertical mode is close to this limit value. It may be useful to utilize friction coefficients of this magnitude in further studies on the oscillatory nature of ENSO.

Acknowledgments

We would like to thank the following persons for providing data: Bob Cheney for his last GEOSAT sea-level product, Klaus Wyrtki and Gary Mitchum for sea level from the TOGA Sea-level Center Data Set, Jim O'Brien and James Stricherz for their FSU wind stress product, and Mike McPhaden for the dynamic height series of three equatorial moorings. Comments from Gerard Eldin, Jay McCreary, Billy Kessler, and Tony Busalacchi are appreciated.

References

Battisti, D.S., and A.C Hirst, 1989: Interannual variability in a tropical atmosphere-ocean model: Influence of the basic state, ocean geometry and nonlinearity. *J. Atmos. Sci.*, 46, 1687-1712.

Busalacchi, A.J., and M.C. Cane, 1985: Hindcasts of sea-level variations during the 1982-83 El Niño. *J. Phys. Oceanogr.*, 15, 213-221.

Busalacchi, A.J., K. Takeuchi, and J.J. O'Brien, 1983: Interannual variability of the equatorial Pacific - Revisited. *J. Geophys. Res.*, 14, 7551-7562.

Cane, M.A., and R.J. Patton, 1984: A numerical model for the low-frequency equatorial dynamics. *J. Phys. Oceanogr.*, 14, 1853-1863.

Cheney, R.E., N.S. Doyle, B.C. Douglas, R.W. Agreen, L. Miller, E.L. Timmerman, and D.C. McAdoo, 1991a: *The Complete GEOSAT Altimeter GDR Handbook*, NOAA Manual NOS NGS, 7, National Ocean Service, Rockville, MD, 79 pp.

Cheney, R.E., W.J. Emery, B.J. Haines, and F. Wentz, 1991b: Recent improvements in GEOSAT altimeter data. *EOS*, 72, 577-580.

Eldin, G., A. Morliere, and G. Reverdin, 1992: Acoustic Doppler current profiling along the Pacific equator from 95°W to 165°E. *Geophys. Res. Letters*, 19, 913-916.

Gent, P.R., K. O'Neill, and M.A. Cane, 1983: A model of the semi-annual oscillation in the equatorial Indian Ocean. *J. Phys. Oceanogr.*, 13, 2148-2160.

Gill, A.E., 1980: Some simple solutions for heat-induced tropical circulation. *Quart. J. Roy. Met. Soc.*, 106, 447-462.

Goldenberg, S.B., and J.J. O'Brien, 1981: Time and space variability of tropical Pacific wind stress. *Mon. Wea. Rev.*, 109, 1208-1218.

Levitus, S., 1982: *Climatological Atlas of the World Ocean*, NOAA Prof. Paper 13, U.S. Govt. Printing Office, Washington, DC, 173 pp.

McCreary, J.P., 1976: Eastern tropical ocean response to changing wind systems: With application to El Niño. *J. Phys. Oceanogr.*, 6, 632-645.

McCreary, J.P., 1981: A linear stratified ocean model of the equatorial undercurrent. *Phil. Trans. Roy. Soc. London*, A298, 603-635.

McCreary, J.P., and D.L.T. Anderson, 1991: An overview of coupled ocean-atmosphere models of El Niño and the Southern Oscillation. *J. Geophys. Res.*, 96, Suppl., 3125-3150.

McPhaden, M.J., and S.P. Hayes, 1990: Moored velocity, temperature, and wind measurements in the equatorial Pacific Ocean: A review of scientific results, 1985-1990. In *International TOGA Scientific Conference Proceedings*, WCRP-43, WMO/TD-No. 379, Geneva, 59-69.

Miller, L., and R. Cheney, 1990: Large-scale meridional transport in the tropical Pacific Ocean during the 1986-1987 El Niño from GEOSAT. *J. Geophys. Res.*, 95, 17,905-17,919.

Neelin, J.D., M. Latif, M.A.F. Allaart, M.A. Cane, W.L. Gates, P.R. Gent, M. Ghil, C. Gordon, N.C. Lau, C.R. Mechoso, G.A. Meehl, J.M. Oberhuber, S.G.H. Philander, P.S. Schopf, K.R. Sperber, A. Sterl, T. Tokioka, J. Tribbia, and S.E. Zebiak, 1992: Tropical air-sea interaction in general circulation models. *Clim. Dyn.*, 7, 73-104.

Sciremammano, F., Jr., 1979: A suggestion for the presentation of correlations and their significance levels. *J. Phys. Oceanogr.*, 9, 1273-1276.

Suarez, M.J., and P.S. Schopf, 1988: A delayed action oscillator for ENSO. *J. Atmos. Sci.*, 45, 3283-3287.

Wakata, Y., and E.S. Sarachik, 1991: Unstable coupled atmosphere-ocean basin modes in the presence of a spatially varying basic state. *J. Atmos. Sci.*, 48, 2060-2077.

Wyrtki, K., 1975: El Niño - the dynamic response of the equatorial Pacific Ocean to atmospheric forcing. *J. Phys. Oceanogr.*, 5, 572-584.

Joel Picaut, Christophe Menkes, Jean-Philippe Boulanger, and Yves du Penhoat
Groupe SURTROPAC
ORSTOM
Noumea, New Caledonia